www.cafetinnova.org

ISSN 0974-5904, Volume 10, No. 03

DOI:10.21276/ijee.2017.10.0316

International Journal of Earth Sciences and Engineering

June 2017, P.P. 577-584

Research of the Numerical Simulation based on Granular Discrete Element Method of Rocky Slopes with Weak Interlayer's under Seismic Loads

CHEN XIAOXUE, XU PEIHUA, ZHANG WEN* AND WANG FEI

College of Construction Engineering, Jilin University, Changchun, 130026, CHINA

Email: *zhang_wen@jlu.edu.cn*

Abstract: *Based on the water conservancy and hydropower projects of the red rock barrier lake in Ludian County, Yunnan Province, this paper describes the simulation of a B1 rock slope model using the discrete element to test the earthquake damage process, the fracture extension process and the stability of rock slopes. This paper also introduced the modeling process, calibration sequence of a micro structure parameter, the determination of uniaxial-biaxial loading rate of numerical tests and seismic loading method. In order to evaluate the stability of slope under nature and seismic state, the convergence of the time-displacement history curve is regarded as the standard of whether the slope is stable. The results of the trial indicated that earthquakes affect the initiation, acceleration, and progression of rock slope failures. The destruction of rock slopes was mainly attributed to tension and shear, so the parameters of shear strength of slope rock mass materials determined the stability of the deformation. Given the stress concentration along the weak rock stratum, a fracture easily formed and expanded into the plastic penetration area from the top surface of the rock slope.*

Keywords: *rocky slope, earthquake, fracture extension, PFC2D numerical simulation*

1. Introduction

Rocky slopes are mainly damaged by collapses and landslides, and their instability mechanism under the effect of earthquakes can be classified as simultaneous type or later-occurrence type. The slope experiences creep deformation under the long-term effects of weathering, self-weight, and the formation of fracture zone. The rapid increase in super-static pore water pressure, which results from the instantaneous actions of an earthquake, the earthquake inertia force, the quantity of joint fissure, and the distribution form, will also influence the buckling failure form of the slope [1–2].

The local and foreign methods for investigating the stability of rocky slopes under dynamic effects mainly include the quasi-static method, the sliding block analysis method, the rigid limit equilibrium method, the numerical simulation method, and the indoor test method. The rigid limit equilibrium method is applied under the assumption that the earthquake load remains constant in the slope, the quasi-static method analyzes the stability of the slope, and the sliding block analysis method applies finite sliding displacement and replaces the safety factor.

However, the numerical simulation method mainly involves finite, boundary, and discrete elements. Laboratory tests generally utilize similar materials and build a physical model for rocky slopes to analyze their dynamic stability. The latter two methods can actually reflect the damage mechanism of seismic oscillation for rocky slopes and the crack extension process [3]. Earthquakes are characterized by their uncertainty and suddenness. Given that the actual time and place of an earthquake cannot be accurately predicted, the damage process of seismic oscillation for slopes under natural conditions cannot be observed and researched in real time. The crack extension process for rocky slopes is related to the frequency and time of dynamic loading and is influenced by changes in amplitude. Therefore, the laboratory dynamic loading test cannot easily realize an analog simulation of seismic waves. Finite element modeling in numerical simulation generally simplifies the rock soil into a homogeneous and linear isotropic body and cannot accurately determine a possible large deformation, slippage, and fall during the earthquake. According to finite difference theory, the numerical simulation method for discrete element considers a medium as a discrete unit and does not consider the continuous deformation. Given that seismic wave propagation is a discrete process, the discrete numerical simulation method has been widely applied in investigating the dynamic damage process of rocky slopes [4].

Based on the field survey data and the PFC2D numerical simulation method for discrete element, this study builds a numerical model for rocky slopes to test the dynamic damage in slopes under seismic effects. During seismic loading, the seismic acceleration magnitude is transformed into force according to Newton's second law and is applied to boundary particles to realize single boundary loading and avoid the reflection effects of seismic waves. The

Received: January 02, 2017; Accepted: May 10, 2017; Published: June 30, 2017
International Journal of Earth Sciences and Engineering, 10(03), 577-584, 2017, DOI:10.21276/ijee.2017.10.0316

test applies a displacement deformation and crack extension monitoring system in PFC to set the monitoring points for displacement deformation in critical positions of the slope as well as to investigate the crack extension process and the instability system of slopes under seismic effects [5].

2. Project Profile and Geological Conditions

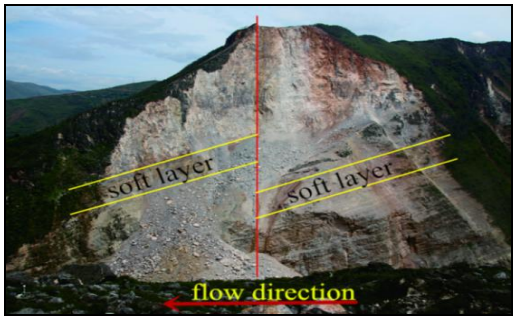

Fig. 1 *Full view of the Hongshiyan collapse*

At 16:30 of 3 August 2014, the Ludian County in Yunnan Province suffered a level 6.5 earthquake, which resulted in the collapse of the right mountain in the main stream of Niulanjiang River at the junction between Lijiang Village, Huodehong Town, Ludian County and Hongshiyan Village, Baogunao Town, Qiaojia County. The collapse resulted in the formation of a barrier lake. The B1 rocky slope is located on the right bank of the downstream Hongshi Barrier Lake in Niulanjiang River (Fig. 1), where multiple long-term crustal movements have occurred and resulted in various forms of structural deformation as well as multiple structural features with different properties, sizes, shapes, and directions. The main structure in this zone is located in the N–E direction, while the nearby structure is located in the S–N direction. The structure at the N–W direction does not grow in this zone and mostly comprises the main tectonic zone at the N–E and nearby S–N directions (Fig. 2).

The lithological characteristics of the exposed stratum include the upper dark gray limestone of Qiaojia Fm with a little dolomite limestone from the mid-Ordovician period (P_{1q}), the middle gray shale and limestone in Liangshang Fm with a sandy conglomerate and inferior coal seam (P_{1L}) that form a soft rock interlayer, and the lower black gray dolomite (D_{2q}).

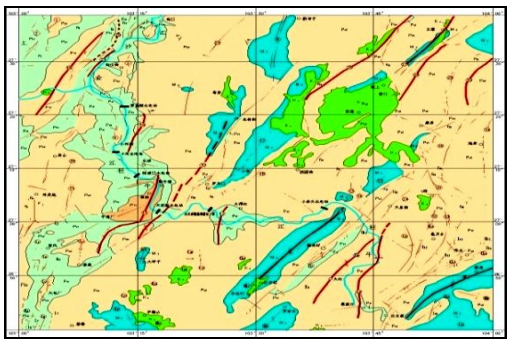

Fig. 2 *Regional seismotectonic map*

The slope is approximately 700 m high and 300 m wide. The landslide mass has a 100 m thickness and a gradient ranging from 70° to 85°. The internal slope joint, crack growth, and joint include three groups, namely, the steep dip joint at the direction of the right-angled stream, the parallel stream, and the bedding joint. Fig. 3 shows the rose diagram of the joint on the site and the pole contour map. According to the field survey, the distribution of joint attitude is highly concentrated and dominantly occurs in the N–E direction. The slope rocks are alternatively distributed, while the soft rocks demonstrate an inhomogeneous deformation under the effect of self-weight load for upper rocks, thereby resulting in cracks and disintegration for the upper fragile rocks. Under seismic effects, the unloading cracks at the parallel stream are combined with other structural surfaces (e.g., bedding joint) to form a sliding boundary, thereby expanding the scope of landslide and collapse. According to field survey, it is mainly landslide form of damage for B1 rocky slope with subsequent collapse. After the landslide, the internal slope is adjusted along with stress, while the unloading cracks on the slope surface massively increase and combine the harmful structure surfaces with the dangerous blocks. The unstable blocks continuously collapse and fall under the influences of aftershock, rainfall, and stress adjustment for slope surfaces. The collapse has a total volume of 1000×10^4 m^3, the mountain collapse along the direction of the river is approximately 890 m long, and the thick wall is approximately 500 m high.

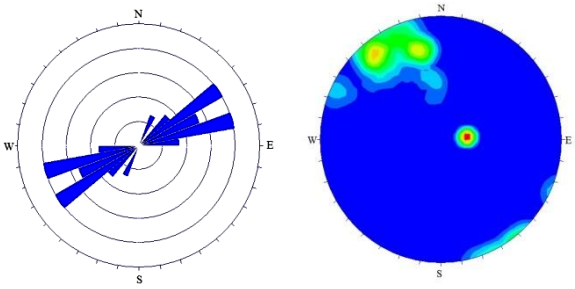

Fig. 3 *The rose diagram of joint and the pole density contour map*

3 Build Slope Model

3.1 Build Discrete Element Model

The plotted longitudinal section of the B1 rocky slope (Fig. 4) is scaled at the ratio of 1:100, and a numerical model for rocky slopes with a height of 7 m and a width of 8 m is built in PFC2D (Fig.5). The layer thickness of Dolomitic limestone, shale, dolomite and weathering is 5.2 m, 0.2 m, 2.6 m and 0.1 m to 0.8 m respectively in the numerical model.

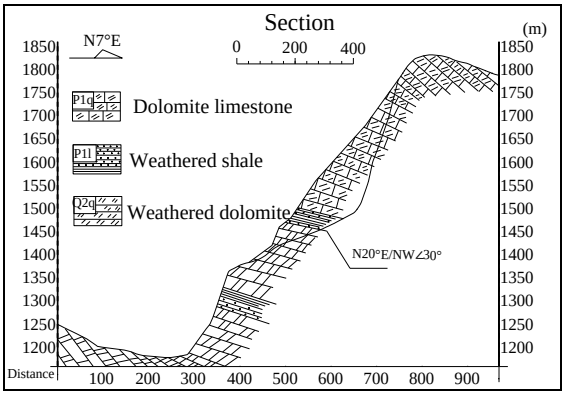

Fig. 4 *B1 slope geological section*

Given that the slope is rocky, a parallel connection model is selected for the particles. To satisfy the calculation accuracy requirements of the numerical model and avoid adverse side effects, the particle size for the packed model must be minimized as much as possible. However, given the limited computing power of the workstation, the quantity of particles must not be too large. The minimum particle size must be 1/40 of the model width in order for the radius of the packed particles to range between 2.5 cm and 4.15 cm. The slope model is cut and generated to delete the surplus particles, form a new slope model, and obtain 15275 particles. The gravitational field is established, and the iterative computation is implemented to obtain a balanced scale model for slope values [6-8]. To study the slope deformation and damage process under seismic effects, a series of displacement monitoring points are designed on an internal slope. Serial displacement monitoring points are designed on potential sliding surfaces to monitor the overall displacement conditions. The B serial monitoring points at the x direction and the C serial monitoring points at the y direction are designed at the middle and slope toe to monitor the internal particles as well as the horizontal and vertical deformation under the effect of seismic waves.

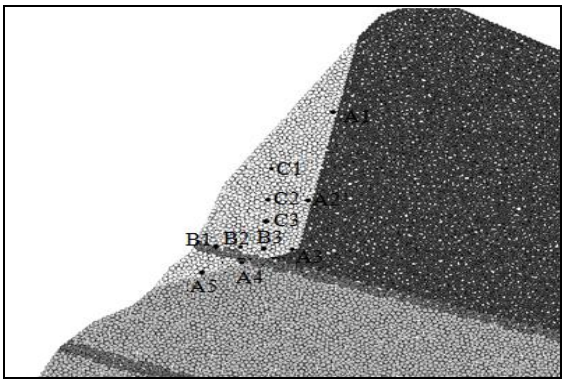

Fig. 5 *Numerical model of B1 rocky slope*

3.2 Select and Determine the Material Parameters

3.2.1 Select the Macro Parameters

In PFC numerical simulation, the macro physical parameters and micro parameters for the particles do not have any direct corresponding relation. Table 2-1 shows the macro physical and mechanic parameters of the B1 rocky slope. The numerical test is performed, and the relation between the macro and micro parameters is established to determine the micro mechanical parameters for granular materials and reflect the actual features of the B1 rocky slope [9].

Table 1 *Macro mechanic parameters of the rock terrain*

Macro parameters	Volume weight ρ Kn/m^3		Elastic modulus E_0 Gpa		Poisson's ratio μ		Internal friction angle φ(°)		Cohesion c Mpa		Strength σ_c Mpa	
	Phy	Num	Phy	Num	Phy	Num	Phy	Num	Phy	Num	Phy	Num
Dolomite limestone P_{1q}	24.0	26.5	12.0	13.0	0.2	0.2	42	27	10.7	12.3	6.5	7.4
Weathered limestone P_{1q+m}	23.5	26.5	5.2	6.3	0.23	0.21	28	24	1.2	2.6	3.8	4.8
Weathered shale P_{1L}	24.6	26.0	2.4	3.2	0.23	0.22	30	26	0.5	1.7	2.4	3.6
Weathered dolomite D_{2q}	26.1	26.5	3.4	4.7	0.22	0.2	37	25	0.8	1.3	3.2	4.2

3.2.2 Calibration of Material Micro Parameters

Uniaxial and biaxial numerical tests are performed to determine the parameters. Samples of 25 cm×50 cm are generated, and then the sensitivity test is conducted for the loading rate. Although a slower loading rate is preferred in numerical tests, such rate will lengthen the computation time. However, a fast loading rate improves the peak strength, shows no linear elasticity for early-stage deformation, and increases the test errors. Therefore, a time sensitivity test for loading rate must be performed before determining the parameters. This research performs a numerical test with uniaxial compression to set different loading rates for the uniaxial compression test and generate stress–strain and strain–time curves under different loading rates as shown in Fig. 6.

The loading rates for the uniaxial compression test are 0.01 m/s, 0.05 m/s, and 0.1 m/s, which corresponding peak strengths are 67.7 MPa, 68.3 MPa, and 69.5 MPa with computation times of 34.81 min, 9.09 min, and 4.37 min, respectively. The loading ratio is inversely

proportional to computation time. According to the stress–strain curve for uniaxial compression under various loading rates, peak strength is not obviously influenced by loading ratio, but shows apparent brittle fracture features; therefore, the identified micro parameters may not actually reflect the mechanical characteristics of rocky materials. When the numerical test is conducted to determine the parameters, the proper loading rate must be selected to guarantee test accuracy. Therefore, 0.05 m/s is selected as the loading rate of Limestone after a series of sensitivity tests. Therefore, the proper loading rate of weathered limestone, shale and dolomite is 0.01 m, 0.01 m and 0.005 m respectively in accordance with the above method. Similar research is provided in reference by Zhang X-P. [11-12].

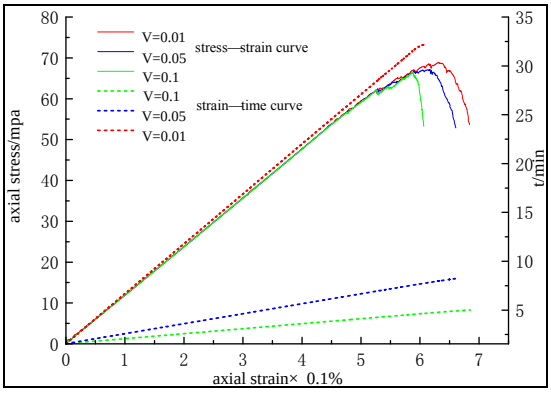

Fig. 6 *Stress–strain–time curves in the uniaxial compression test*

The elastic modulus, Poisson's ratio, cohesion, and internal friction angle are determined in the numerical test for PFC. A uniaxial test is generally conducted to determine the strength parameters of weathered rocks. Young's modulus is mainly influenced by the contact modulus and parallel bonding modulus, while Poisson's ratio is mainly influenced by the contact stiffness ratio of particles and the parallel bonding ratio of stiffness. In each of these tests, the normal and tangential strength parameters in the parallel bonding model must be adjusted to a certain proportion to determine quickly the proper scope of the parameters. The standard deviation does not have an apparent influence on peak strength, but has obvious influences on the material damage model. Therefore, the mean values of normal strength and cohesion must maintain a ratio of 4:1 with standard deviation to use the same damage model for each test. However, given that numerous micro parameters influence and restrict one another, the parameters must be combined and adjusted in the numerical test [13-14].

This research performs a uniaxial numerical test to determine the elastic modulus, Poisson's ratio, and uniaxial compressive strength. A biaxial compression test is also conducted under the confining pressures of 5 MPa, 10 MPa, and 15 MPa. The Mohr's circle for stress is drawn under the corresponding parameters to determine the cohesion and internal friction angle and to identify the micro parameters of rocks (Table 2). The numerical samples have no micro cracks, thereby resulting in large deviations in the measured data.

Table 2. *Macro mechanic parameters of the rock terrain*

Micro-parameters	Limestone (P_{1q})	Weathered limestone (P_{1q+m})	Weathered shale (P_{1L})	Weathered dolomite (D_{2q})
Particle density Kg/m^3	2650	2650	2600	2650
Minimum particle radius R_{min} (m)	0.02	0.025	0.025	0.025
Radius ratio R_{max}/ R_{min}	1.66	1.66	1.66	1.66
Loading rate m/s	0.05	0.01	0.01	0.005
Particle contact modulus E_C(Gpa)	8×10^9	3.5×10^9	1.5×10^9	2.0×10^9
Contact Stiffness ratio k_n/k_s	1.27	1.5	1.35	1.37
Friction coefficient f_c	0.35	0.25	0.15	0.2
Parallel bond modulus E_b(Gpa)	8×10^9	3.5×10^9	1.5×10^9	2.0×10^9
Stiffness ratio of parallel bond k_{nb}/k_{sb}	1.27	1.5	1.35	1.37
Normal strength of parallel bond (pa)	60×10^6	32×10^5	20×10^5	25×10^5
Standard deviation of strength for parallel bond (pa)	15×10^6	8×10^5	5×10^5	6.25×10^5
Cohesion pb_ten (pa)	45×10^6	25×10^5	16×10^5	18×10^5
Standard deviation of cohesion (pa)	11.25×10^6	6.25×10^5	4×10^5	4.75×10^5
Internal friction angle pb_fa (°)	45	32	23	27

Therefore, various parameters must be slightly adjusted when being determined in the PFC numerical test.

3.3 Seismic wave load

The boundary treatment for the numerical model of the slope cannot be easily achieved for PFC dynamic loading. In the PFC numerical model for the slope, seismic waves are mainly loaded by (1) providing a changed speed for the model boundary wall and (2) by applying force on the boundary particle units. However, this research transforms the seismic acceleration magnitude into force. First of all, the corresponding fish functions are used to traversal all boundary particles and read their mass. So that

seismic acceleration values are converted into force according to Equation. 1. Then the force is applied to the boundary particles [15-16].

$$\sigma_n = -2(\rho C_p)\, v_n \quad (1)$$

Where,

$$C_p = \sqrt{\frac{K+4G/3}{\rho}} \quad (2)$$

Where,

$$K = \frac{E}{3(1-2\mu)} \quad (3)$$

$$G = \frac{E}{2(1+\mu)} \quad (4)$$

Where, σ_n is the normal stress. ρ, C_p is density and wave velocity of medium. v_n is particle velocity in the vertical direction. K, G, E is bulk Modulus, shear Modulus and elastics Modulus. μ is Poison's ratio.

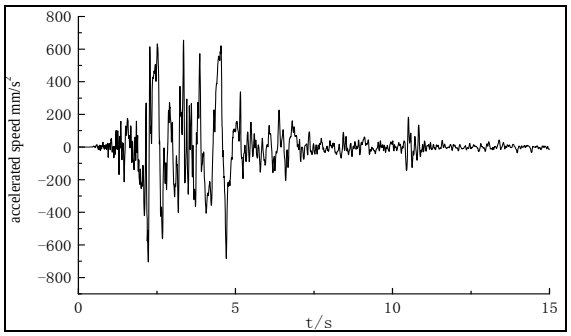

Fig. 7 *Curve of earthquake acceleration in Ludian County, Yunnan Province*

This research deletes the boundary wall of the slope model, and fixes the displacement at the y direction for the left and right boundary particles to apply force at the x direction. The displacement at the x direction for the bottom boundary particles is fixed in order to apply force at the y direction and effectively avoid the reflection effect for the loading seismic waves by using the application wall. As shown in the acceleration–time curve within 15 s before the level 8.03 earthquake in Ludian County (Fig. 7), this seismic wave only has one wave crest zone and a later aftershock is not apparent. To save computation time for the numerical model, this research only selects the acceleration values of the previous 12 s seismic oscilaltion to conduct the dynamic loading test for the B1 rocky slope model.

4 Analysis of the simulation results of the slope destruction process

4.1 Analysis of the stability of rocky slopes under the effect of gravity

In the numerical simulation, when the rocky slope is under a stable condition, the end of the displacement–time curve for the monitoring points at the potential sliding surface and the slope is placed under the convergence condition. By contrast, when the slope loses its stability, the displacement–time curve is placed under the scattered condition. According to the parallel connection condition for slope particles as shown in Fig. 8, under the natural effects of gravity for slopes before an earthquake, the weak intercalated layer at the foot of the slope forms an apparent stress concentration zone to damage the particle connection. The internal slope gradually forms micro cracks, but the end of the displacement–time curve at the critical positions shown in Fig. 9 is placed under the convergence condition, thereby indicating the stable condition of the slope. Therefore, the internal section of the B1 rocky slope does not generate large-scale deformation and unstable damage for overall sliding before the earthquake (under natural conditions) and its form can be completely maintained. These findings are consistent with the survey results.

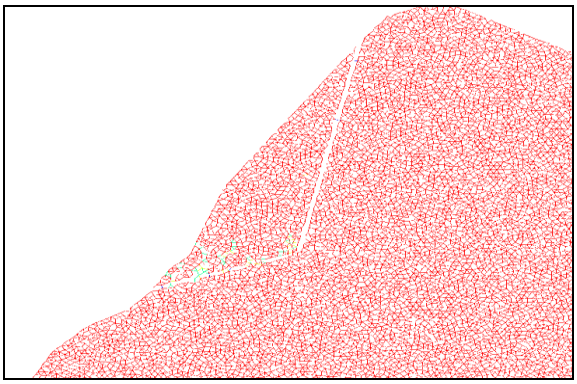

Fig. 8 *Parallel bond position of the particles before the earthquake*

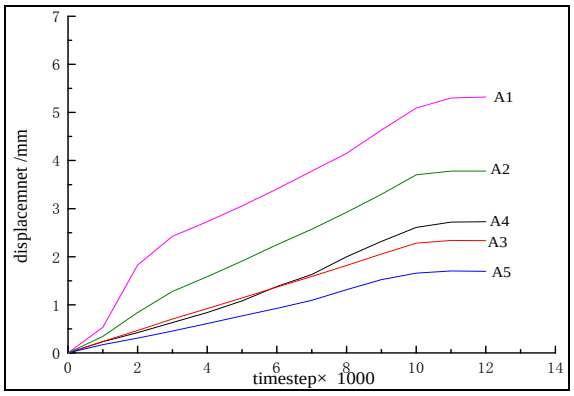

Fig. 9a *Time history curves of displacement*

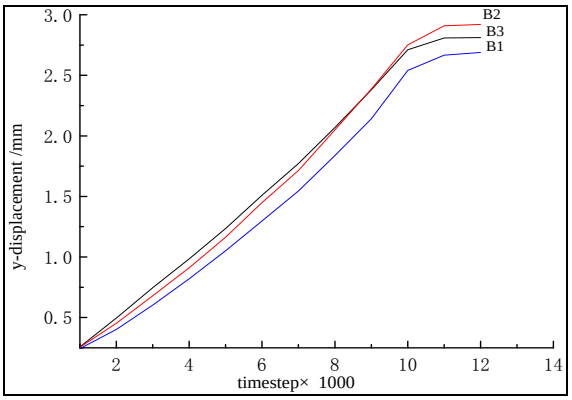

Fig. 9b *Time history curves of y-displacement, continued*

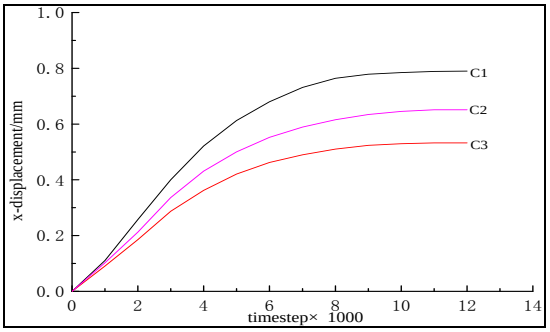

***Fig. 9c** Time history curves of y-displacement, continued*

4.2 Analysis of the stability of rocky slopes under the effect of earthquake

When a seismic load is applied on the rock slope, the parallel connection conditions at 2 s, 4 s, 6 s, 8 s, 10 s and 12s are changed as shown in Figs. 10a to 10f. According to the changes shown in Figs. 10a to 10c, given the effects of seismic force and within 6 s before loading the seismic wave, the connection among particles generates fracture and damage along the original weak face at the slope feet that extend to the internal slope and surface. The internal slope has several broken faces, and the bearing capacity and stability of the slope rapidly decline. Figs. 10a and 10b show that the internal slope cracks rapidly extend and that seismic loading produces activation and acceleration effects on the damage for rocky slopes. In other words, the instantaneous and dynamic effects greatly influence the slope stability. Given the increased amplitude of the seismic wave, the quantity of cracks continuously increases and extends to the top of the slope, and several cracks converge and form a crack network. When the rocks are cut, the damage of the overall slope rock increases and forms a connecting and plastic flow zone, thereby gradually losing the completeness of the slope.

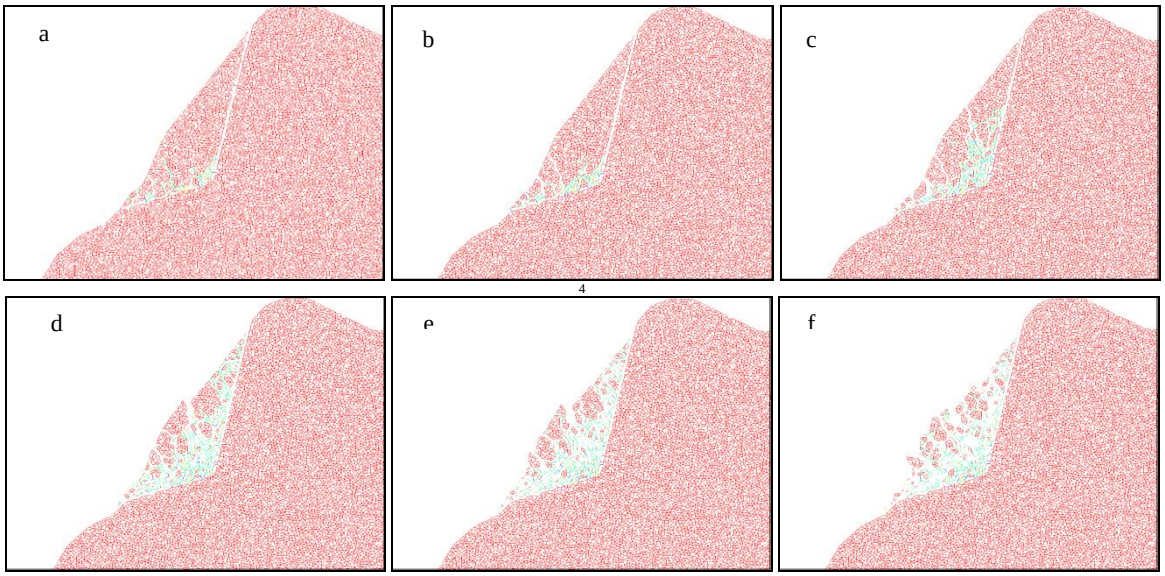

***Fig. 10** Analysis of the landslide mechanism in the earthquake process*

According to the analysis and comparison of the displacement–time curves in Figs. 9 and 11, the convergence degrees for the curves at the x and y directions differ before and after the earthquake. The curvature rapidly increases for the displacement–time curve at the y direction, but no such increase is observed in the curve at the x direction. These observations indicate that vertical deformation forms in the internal slope before the earthquake under the effect of gravity. After the earthquake, the curvature rapidly increases at the x direction and no obvious increase is observed in the y direction. In other words, under the short-term effect of seismic loading, the rocky slope generates lateral tension and shear fracture (i.e., lateral shear and deformation displacement). When the loading ends, the displacement–time curve becomes scattered and the accumulated displacement for the slope reaches a certain value, thereby resulting in permanent deformation. Therefore, the slope is placed under an unstable condition.

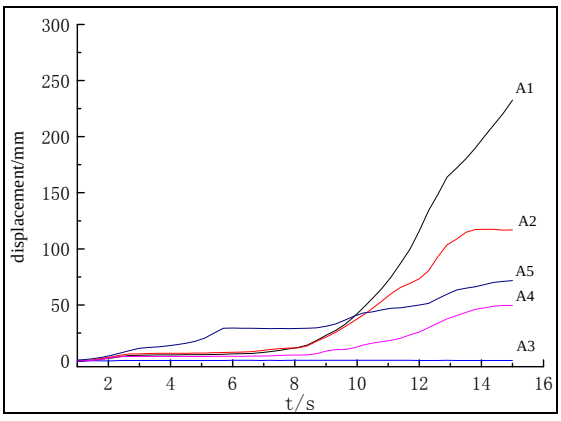

***Fig. 11a** Time history curves of displacement*

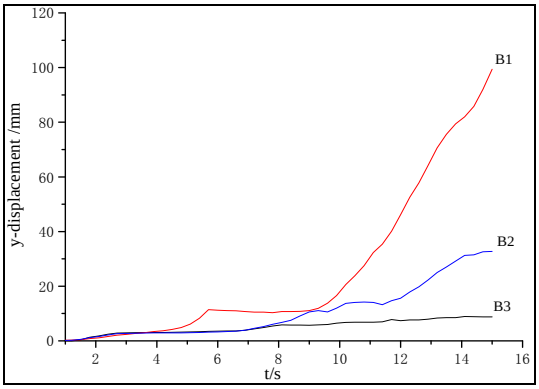

Fig. 11b *Time history curves of y-displacement*

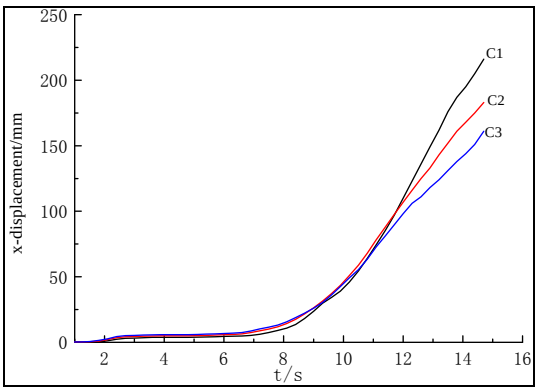

Fig. 11c *Time history curves of y-displacement*

5. Conclusions

(1) Earthquakes produce three effects on internal rocky slopes, namely, activation, acceleration, and accumulated damage effects. The corresponding damage processes include the deformation and slow-motion stage, the fierce loading stage, and the instability damage stage. The numerical simulation shows that the level 8.05 earthquake in Ludian County produced all three effects on the B1 rocky slope of the barrier lake in Niulanjiang River. Therefore, seismic oscillation is a key factor in the damage mechanism and stability analysis of rocky slopes.

(2) The stability of rocky slopes with weak bedding is usually controlled by the strength of the bedding. The weak bedding easily forms stress concentration under the effect of seismic loading, thereby resulting in tension and shear damage and gradually forming a connected shaping zone. The fracture surface extends to the slope surface and along the weak surface. Therefore, under the effect of seismic loading, the shearing resistance and strength of extension for rocky slopes are important conditions to determine the stability of these slopes.

(3) When the discrete element is applied for a related numerical simulation, the time sensitivity test for loading rate must be performed when determining the micro parameters to select a proper loading rate for the uniaxial and biaxial test, save time for determining parameters, reduce errors, and improve the reliability of the numerical simulation. The B1 slope simulation results are consistent with those of the field survey. Therefore, discrete element PFC2D is beneficial in studying the dynamic damage process and crack extension mechanism of rocky slopes.

References

[1] Wang Qian. Study on deformation characteristics and failure mechanism of bedding rock slope under earthquake [D]. JinLin University, 2010.

[2] Collop, A.C., G.R. McDowell and Y.W. Lee, Modelling dilation in an idealised asphalt mixture using discrete element modeling [J]. Granular Matter, 8(3), PP.175-184, 2006, DOI: 10.1007/s10035-006-0013-3.

[3] Zhu Dong. The analysis of the stability of bedding slope under the errect of earthquake [D].Southwest Jiaotong University 2012.

[4] Ai, J., P.A. Langston and H.S. Yu, Discrete element modelling of material non‐coaxiality in simple shear flows [J]. International Journal for Numerical & Analytical Methodsin Geomechanics, 38(6), PP.615-635, 2014, DOI: 10.1002/nag.2230.

[5] Cai, W., G.R. McDowell and G.D. Airey, Discrete element modelling of uniaxial constant strain rate tests on asphalt mixtures. Granular Matter [J], 15(2), 2013, PP.163-174. DOI:10.1007/s10035-013-0396-x.

[6] Zhou Bo, Wang Huabin, Zhao Wenfeng, Li Jiwei, Zheng Bican. Analysis of relationship between particle mesoscopic and macroscopic mechanical parameters of cohesive materials [J].Rock and Soil Mechanics, 33(10), PP. 3171-3178, 2012, DOI:10.16285/j.rsm.2012.10.019.

[7] Xu Yongfu, Xi Yue,Feng Xingbo,Zhu Honggao,Chu Feifei.Simulatioin of Rock Grain Breakage Using PFC^{2D}[J].Journal of Engineering Geology, 0(4), PP.589-596, 2015, DOI:10.13544/j.cnk.jeg.2015.04.001.

[8] Lim, W.L. and G.R. McDowell, Discrete element modeling of railway ballast. Granular Matter, 7(1): PP.19-29, 2005, DOI: 10.1007/s10035-004-0189-3.

[9] Cui Tiejun,Ma Yundong,Wang Laigui. Simulation and analysis of earthquake stability for open-pit coal mine slope with complex structural surface [J] Earthquake engineering and engineering dynamics, 01(1), PP.200-206, 2016, DOI:10.13197/j.eeev.2016.01.200.cuitj.026.

[10] Yang Bing. Granular Simulation on the Process of Slope Failure and Collapse under Seismic Load [D].Tsinghua University, 2011.

[11] Zhang X-P, Wong L N Y. Choosing a proper loading rate for bonded-particle model of intact rock [J]. International Journal of Fracture, 189(2), PP.163-179,2014,.DOI:10.1007/s10704-014-9968-y.

[12] Zhang X P, Wong L N Y. Loading rate effects on cracking behaviour of flaw-contained specimens

under uniaxial compression [J]. International Journal of Fracture, 180(1), PP.93-110, 2013, DOI: 10.1007/s10704-012-9803-2.

[13] Liu Yunpeng, Deng Hui,Huang Runqiu,Song Jinlong.Yuan Jinke. Numerical simulation of seismic response of anti-dumping rock slope interbedded by hard and soft layers [J]. Hydrogeology & Engineering Geology, 39(3), PP.30-37, 2012, DOI:10.16030/j.cnki.issn.1000-3665.2012.03.007.

[14] Li Xinpo, He Siming. Numerical Analysis of the Failure of Heavily Jointed Rock Slopes Using PFC2D [J]. Journal of SiChuan University Engineering Science Edition, 42(S1), PP. 70-75, 2010, DOI:10.15961/j.jsuese.2010.s1.019.

[15] Shi Chong,Wang Shengnian,Liu Lin.Research of Avalanche disaster Numerical Simulation based on Granular Discrete Element method of High-steep Slope under Seismic Loads[J]. Chinese Journal of Rock Mechanics and Engineering, 31(S1), PP.2798-2805, 2013, ISSN: 10006915.

[16] Cui Fangpeng, Hu Ruilin, Yin Yueping, Xu Qiang, Zhang Ming. Discrete Element analysis of Collapsing and Sliding response of Slope Triggered by time difference Coupling effects of P and S Seismic Waves-taking Tang Jiashan Landslide in Beichuan county for example[J]. Chinese Journal of Rock Mechanics and Engineering, 29(2), PP.319-327, 2010, ISSN:10006915